AD-A137 859 PULLOUT OF A RIGID INSERT ADHESIVELY BONDED TO AN ELASTIC HALF PLANE(U) FRANK J SEILER RESEARCH LAB UNITED STATES AIR FORCE ACADEMY CO G K HARITOS ET AL. DEC 83 FJSRL-TR-83-0017 1/1

UNCLASSIFIED F/G 20/11 NL

END
FILMED
3-84
DTIC

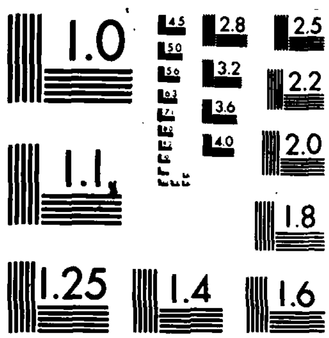
1.0
2.8
2.5
3.2
2.2
3.6
4.0
2.0
1.1
1.8
1.25
1.4
1.6

FRANK J. SEILER RESEARCH LABORATORY

FJSRL-TR-83-0017 DECEMBER 1983

PULLOUT OF A RIGID INSERT ADHESIVELY BONDED TO AN ELASTIC HALF PLANE

FINAL REPORT

GEORGE K. HARITOS

LEON M. KEER

PROJECT 2308-F1

APPROVED FOR PUBLIC RELEASE;
DISTRIBUTION UNLIMITED.

AIR FORCE SYSTEMS COMMAND

UNITED STATES AIR FORCE

This document was prepared by the Department of Engineering Mechanics, USAF Academy Faculty, USAF Academy, Colorado Springs, CO. The research was sponsored by the Frank J. Seiler Research Laboratory.

When U.S. Government drawings, specifications or other data are used for any purpose other than a definitely related government procurement operation, the government thereby incurs no responsibility nor any obligation whatsoever, and the fact that the government may have formulated, furnished, or in any way supplied the said drawings, specifications, or other data is not to be regarded by implication or otherwise, as in any manner licensing the holder or any other person or corporation or conveying any rights or permission to manufacture, use or sell any patented invention that may in any way be related thereto.

Inquiries concerning the technical content of this document should be addressed to HQ USAFA/DFEM, USAF Academy, Colorado Springs, CO 80840. Phone AC (303) 472-2196.

This report has been reviewed by the Commander and is releasable to the National Technical Information Service (NTIS). At NTIS it will be available to the general public, including foreign nations.

This technical report has been reviewed and is approved for publication.

George K. Haritos

GEORGE K. HARITOS, Major, USAF
Project Engineer/Scientist

Thomas E. Kullgren

THOMAS E. KULLGREN, Lt Col, USAF
Professor and Acting Head,
Department of Engineering Mechanics

Kenneth E. Siegenthaler

KENNETH E. SIEGENTHALER, Lt Col, USAF
Chief Scientist

T. Saito

THEODORE T. SAITO, Lt Col, USAF
Commander

Copies of this report should not be returned unless return is required by security considerations, contractual obligations, or notice on a specific document.

Printed in the United States of America. Qualified requestors may obtain additional copies from the Defense Technical Information Center. All others should apply to: National Technical Information Service
6285 Port Royal Road
Springfield, Virginia 22161

2a. SECURITY CLASSIFICATION AUTHORITY	3. DISTRIBUTION/AVAILABILITY OF REPORT Approved for Public Release Distribution Unlimited
2b. DECLASSIFICATION/DOWNGRADING SCHEDULE	
4. PERFORMING ORGANIZATION REPORT NUMBER(S) FJSRL-TR-83-0017	5. MONITORING ORGANIZATION REPORT NUMBER(S)
6a. NAME OF PERFORMING ORGANIZATION Department of Engineering Mechanics 6b. OFFICE SYMBOL (If applicable) USAFA/DFEM	7a. NAME OF MONITORING ORGANIZATION
6c. ADDRESS (City, State and ZIP Code) USAF Academy Colorado Springs, Colorado 80840	7b. ADDRESS (City, State and ZIP Code)
8a. NAME OF FUNDING/SPONSORING ORGANIZATION Frank J. Seiler Research Lab 8b. OFFICE SYMBOL (If applicable) FJSRL/NA	9. PROCUREMENT INSTRUMENT IDENTIFICATION NUMBER
8c. ADDRESS (City, State and ZIP Code) USAF Academy Colorado Springs, Colorado 80840	10. SOURCE OF FUNDING NOS.

PROGRAM ELEMENT NO.	PROJECT NO.	TASK NO.	WORK UNIT NO.
612308 61102F	2308	F1	

11. TITLE (Include Security Classification) Pullout of a Rigid Insert Adhesively Bonded to an Elastic Half Plane (U)

12. PERSONAL AUTHOR(S) George K. Haritos, AFIT; Leon M. Keer, Northwestern University

13a. TYPE OF REPORT	13b. TIME COVERED	14. DATE OF REPORT (Yr., Mo., Day)	15. PAGE COUNT
Final	FROM Apr 81 TO Dec 83	December 1983	29

16. SUPPLEMENTARY NOTATION

17. COSATI CODES			18. SUBJECT TERMS (Continue on reverse if necessary and identify by block number)
FIELD	GROUP	SUB. GR.	Rigid Insert; Elastic Half Plane; Adhesive Bonding; Shear and Normal Stresses; Shear Pullout; Edge Crack; Crack Opening Displacements
?	11		

19. ABSTRACT (Continue on reverse if necessary and identify by block number)

The problem of a finite, rigid fiber which is partially embedded in and adhesively bonded to an elastic half plane is considered within the context of plane elastostatics. Loading is applied to this insert so that it translates in the vertical direction without rotation. Of interest here are the shear and normal stresses generated along the bonded interface that will cause the adhesive to undergo both shear and normal deformation. It is assumed that throughout this deformation the adhesive behaves as a linearly elastic material.

Two distinct mixed boundary value problems are formulated: the shear pullout one, already described, and an opening problem, described next. The opening problem assumes an edge crack in the half plane subjected to opening pressure, equal in magnitude to the normal stress distribution generated by the pullout problem. The physical quantities of interest in this problem are the crack opening displacements.

(Continued on Reverse)

20. DISTRIBUTION/AVAILABILITY OF ABSTRACT UNCLASSIFIED/UNLIMITED ☒ SAME AS RPT. ☒ DTIC USERS ☐	21. ABSTRACT SECURITY CLASSIFICATION UNCLASSIFIED
22a. NAME OF RESPONSIBLE INDIVIDUAL George K. Haritos	22b. TELEPHONE NUMBER (Include Area Code) 513-255-2998/3517 22c. OFFICE SYMBOL AFIT/ENY

Block 19 Continued:

The problems considered here can be viewed as appropriate idealizations for studying two separate, yet similar, classes of engineering problems. Within the context of plane strain, they would be appropriate for investigating interface failure in fiber reinforced composite materials. In the generalized plane stress context, they deal with finite rigid inserts of negligible width embedded in and adhesively bonded to a semi-infinite elastic sheet. The formulation of these problems leads to governing singular integral or integrodifferential equations. Numerical results are obtained via a technique by Gerasoulis and Srivastav.

PULLOUT OF A RIGID INSERT ADHESIVELY

BONDED TO AN ELASTIC HALF PLANE

by

G.K. Haritos

Department of Aeronautics and Astronautics

Air Force Institute of Technology

Wright Patterson Air Force Base, Ohio 45433

and

L.M. Keer

Department of Civil Engineering

Northwestern University

Evanston, Illinois 60201

Abstract

The problem considered here is that of a finite, rigid insert partially embedded in and adhesively bonded to an elastic half plane. Two distinct problems are investigated: the shear pullout of the insert without rotation, which takes into account the adhesive's resistance to shear deformation, and an opening problem which incorporates the adhesive's resistance to normal deformation. This latter problem assumes the presence of an edge crack in the half plane subjected to opening pressure which equals in magnitude the normal stress distribution due to the pullout problem. These mixed boundary value problems are governed by singular integral or integrodifferential equations. Numerical results are obtained via a technique introduced by Gerasoulis and Srivastav. Several important physical quantities are calculated, such as the shear and normal stress distributions along the bonded interface, and the crack opening displacements.

1. Introduction

The problem of a rigid insert partially embedded in and adhesively bonded to an elastic half space is considered within the context of plane elastostatics. The thickness of the insert is assumed to be negligible. It is also assumed that the adhesive's deformation remains in the linear elastic range. The thickness of the adhesive is small, but not negligible.

Loading is applied to this insert so that it translates in the vertical direction without rotation (Fig. 1). Of interest here are the shear and normal stresses generated along the bonded interface. These stresses will cause the adhesive to undergo both shear and normal deformation. Two distinct problems are considered: the shear pullout problem already described, which takes into account the adhesive's resistance to shear deformation, and the opening problem, described next, which considers the adhesive's resistance to normal deformation. The opening problem assumes an edge crack in a half space subjected to opening pressure which is equal in magnitude to the normal stress distribution resulting from the pullout problem. In this case, the adhesive material's resistance to normal deformation is used to reduce the opening pressure's intensity. The physical quantities of interest in this problem are the crack opening displacements.

The problems considered here can be viewed as appropriate idealizations for studying two separate, yet similar, classes of problems. In the context in which they have been presented thus far, they are problems in plane strain. As such, they are appropriate for investigating the mechanics of interface failure in fiber-reinforced composite materials. The more realistic case of adhesive failure (adhesive material allowed to deform non-linearly) is currently being considered by the authors. As pointed out by Brussat and

Westmann [1] and by Chamis [2], interface damage is believed to be one of the earliest forms of damage in such composite materials. The subject of fiber debonding has attracted several investigators over the last several years (see [1], [2] for summary). One fundamental question that seems to remain still unanswered, and which is addressed in this paper, is whether the surfaces of a crack at the fiber-matrix interface are traction-free, or remain in contact. It is suggested in [1] that the debonded surfaces may be open or closed depending on the relative magnitude of the applied versus the residual stresses.

In the generalized plane stress context, these problems deal with finite rigid inserts of negligible width, partially embedded within a semi-infinite elastic sheet. In this case, the results obtained may serve to better understand the stress distribution at the bonded interface of dissimilar materials, where one is significantly more rigid than the other. More importantly, an extension of this work which will be addressed in the near future will consider the case of an elastic insert of finite width embedded in an elastic half plane. That problem would be applicable to several physical situations, such as the primary adhesively bonded aircraft fuselage being considered by the U.S. Air Force [3].

The problems are formulated as mixed boundary value problems. This leads to singular integral or integrodifferential equations, which are solved numerically for the desired physical quantities by use of a numerical technique introduced by Gerasoulis and Srivastav [4], [5]. The material constants selected for the adhesive and for the adherend material correspond to materials commercially available.

2. Formulation and Basic Equations

The formulation of the problems considered in this investigation makes use of certain results obtained in two earlier papers [6], [7]. Those papers considered the problem of a finite, rigid block embedded in an elastic half space [6], and that of a rectangular trench in an elastic half plane [7]. The problems were formulated by superposition of the solutions for rigid line inclusions and cracks, respectively, parallel and perpendicular to the free surface of the half plane. The results which pertain to the present work are those derived in [6] for a rigid line inclusion perpendicular to the free surface of the half plane, and the ones derived in [7] for an edge crack.

A. Rigid Insert Pullout: The Shear Mode

A rigid line inclusion is partially embedded in and bonded to an elastic half plane, $y>0$, so that it occupies the line segment $0\leq y\leq h$, $x=0$ in the half plane. The inclusion is loaded by a force P acting along the negative y-axis as shown in Fig. 1. The material properties of the half plane are taken as μ and κ; μ is the shear modulus, while κ is related to Poisson's ratio ν by $\kappa = 3-4\nu$ (plane strain), or $\kappa = (3-\nu)/(1+\nu)$ (generalized plane stress). The inclusion is assumed to be bonded to the half plane by use of some adhesive material in such a manner that there are no discontinuities in the application of the adhesive to the inserted inclusion, and no significant variations in its thickness, which is also assumed to be negligibly small (less than 5×10^{-3} in.). The adhesive is assumed to behave as a number of linear springs, subjected to shear in this case. The stiffness of these springs, k_s, is computed using the mechanical properties of the adhesive.

This is discussed in detail in a later section.

The shear stress developed in the adhesive (and transferred to the half plane) may be written as follows:

$$\tau_{xy}(x,y) = k_s \left[u_y(x,y) - u_0\right] \; ; \quad x = 0, \quad 0 \leq y \leq h \tag{2.1}$$

Here, u_0 is a constant representing the y-displacement of the rigid inclusion, while u_y designates the y-displacement of the half plane material. Thus, the quantity in the brackets gives the displacement of the insert relative to the half plane, which is also the shear deformation of the adhesive. The constant k_s is, as defined earlier, the stiffness of the adhesive modeled as a shear spring.

The displacement u_0 cannot be calculated. Differentiation of (2.1) with respect to y yields the following equation:

$$\frac{\partial}{\partial y}\left[u_y(x,y)\right] = \frac{1}{k_s}\frac{\partial}{\partial y}\left[\tau_{xy}(x,y)\right] \; ; \quad x = 0, \quad 0 \leq y \leq h \tag{2.2}$$

The right-hand side of eqn (2.2) is given in terms of a singular integral equation derived in [6] using integral transform techniques [8], [9]. When that result is used, equation (2.2) takes on the following form:

$$\frac{1}{4\pi(\kappa+1)} \left\{ 2\kappa \int_0^h \frac{D(t)dt}{y-t} + \int_0^h D(t) \left[\frac{(\kappa-1)^2}{y+t} - \frac{2[2t-\kappa(y+t)]}{(y+t)^2} \right.\right.$$

$$\left.\left. + \frac{8yt}{(y+t)^3} \right] dt \right\} = \frac{1}{k_s}\frac{\partial}{\partial y}\left[\tau_{xy}(x,y)\right] \; ; \quad x = 0, \quad 0 \leq y \leq h \tag{2.3}$$

The function $D(y)$ is the unknown shear stress discontinuity associated with the rigid inclusion and it is defined as follows:

$$D(y) = \tau_{xy}^{(2)} - \tau_{xy}^{(1)} \quad ; \quad x \geq 0, \quad 0 \leq y \leq h \tag{2.4}$$

The superscripts (1) and (2) denote the regions to the left and to the right of the inclusion, respectively. The symmetry of the problem requires that $\tau_{xy}^{(2)} = -\tau_{xy}^{(1)}$. Clearly then, the following relatic must hold between τ_{xy} and D:

$$\tau_{xy}(0,y) = \frac{1}{2} D(y) \; ; \qquad 0 \leq y \leq h \tag{2.5}$$

Substitution of eqn (2.5) into eqn (2.3) leads to the following integrodifferential equation in the unknown D(y):

$$\int_0^h \frac{D(t)dt}{t-y} + \int_0^h D(t)K(y,t)dt = -\frac{\pi(\kappa+1)\mu}{\kappa k_s} \frac{\partial}{\partial y} [D(y)] \; ; \; x=0, \; 0 \leq y \leq h \tag{2.6}$$

Here, the function K(y,t) is given as follows:

$$K(y,t) = -\frac{1}{2\kappa} \left[\frac{(\kappa-1)^2}{y+t} - \frac{2[2t-\kappa(y+t)]}{(y+t)^2} + \frac{8yt}{(y+t)^3} \right] \tag{2.7}$$

It should be noted here that the expression for $\frac{\partial}{\partial y} u_y$ substituted in eqn (2.2) to obtain eqn (2.3) was derived in [6] so that the following conditions are satisfied:

$$\left.\begin{aligned} u_x^{(2)} - u_x^{(1)} = 0 \\ u_y^{(2)} - u_y^{(1)} = 0 \end{aligned}\right\} \quad x = 0, \quad 0 \leq y \leq h \; ; \tag{2.8}$$

$$\tau_{yy} = \tau_{xy} = 0 \; ; \quad y = 0, \quad 0 \le |x| < \infty \tag{2.9}$$

Equation (2.8) requires that the displacements on either side of the inclusion be continuous, while eqn (2.9) clears the half plane surface of stresses.

Equilibrium in the y-direction is satisfied by requiring that the following relationship hold:

$$\int_0^h D(y)\, dy = P \tag{2.10}$$

Thus, the solution of the shear pullout of the rigid insert problem consists of solving the governing integrodifferential equation (2.6) for the unknown $D(y)$ subject to the equilibrium condition (2.10). The solution is obtained by means of numerical methods as will be discussed in the numerical analysis section.

Once $D(y)$ has been determined the stresses generated along the bond line are readily obtained. The shear stresses are computed using eqn (2.5), while the normal stresses are obtained from the following [6]:

$$\tau_{xx}(0,y) = \frac{\kappa-1}{2\pi(\kappa+1)} \left\{ \int_0^h \frac{D(t)dt}{t-y} + \int_0^h D(t)\, L(y,t)\, dt \right\} ; \; 0 \le y \le h \tag{2.11}$$

The function $L(y,t)$ is defined as:

$$L(y,t) = \frac{1}{\kappa-1} \left[\frac{3\kappa-1}{y+t} + \frac{2(3t-\kappa y)}{(y+t)^2} - \frac{8yt}{(y+t)^3} \right] \tag{2.12}$$

B. Rigid Insert Pullout: The Opening Mode

The normal stress distribution generated along the bond line of the insert during pullout is now applied as opening pressure on an edge crack in the half plane. It is assumed that the crack extends from $y=0$ to $y=h$ and it is located at the bond line, $x=0$. The adhesive material in this case behaves as a number of linear springs of stiffness k subjected to tension. Thus, it resists the opening of the crack by providing a stress equal to k(COD/2) which reduces the intensity of the applied opening pressure. The crack opening displacement (COD) is the distance between the crack surfaces.

The normal stresses within a half plane containing an edge crack are given in [7]. The bond line stresses are given in terms of the dislocation density B(y) as:

$$\tau_{xx}^{c}(0,y) = \frac{2\mu}{\pi(\kappa+1)} \{\int_0^h \frac{B(t)dt}{t-y} + \int_0^h B(t) [\frac{1}{y+t} + \frac{2t(y-t)}{(y+t)^3}] dt\} ; 0 \leq y \leq h \tag{2.13}$$

Here, μ and κ are the half space material constants given earlier. The superscript c is used to distinguish these normal stresses from the ones associated with the shear pullout problem. The dislocation density B(y) is defined as:

$$B(y) = \frac{\partial}{\partial y} [u_x^{(2)} - u_x^{(1)}] ; \quad x = 0, \quad 0 \leq y \leq h \tag{2.14}$$

The superscripts (1) and (2) refer to the half plane regions to the left and to the right of the crack, respectively. The singular integral equation (2.13) was derived in [7] using integral transform techniques.

The governing equation for this problem is formulated by replacing $\tau_{xx}{}^{c}$

in eqn (2.13) by the difference between the opening pressure and the spring induced resisting stress. This leads to the following equation:

$$\int_0^h \frac{B(t)dt}{t-y} + \int_0^h B(t) \left[\frac{1}{y+t} + \frac{2t(y-t)}{(y+t)^3} \right] dt$$

$$= \frac{\pi(\kappa+1)}{2\mu} \left[-\tau_{xx}(0,y) + k\left(\frac{COD}{2}\right)\right] ; \quad x=0, \ 0 \leq y \leq h \qquad (2.15)$$

As stated earlier, the opening pressure τ_{xx} is the one obtained from the shear pullout case, and k is the equivalent spring constant for the adhesive. Following eqn (2.14) the crack opening displacement at y is given by:

$$COD(y) = [u_x^{(2)} - u_x^{(1)}]_y = -\int_y^h B(t)dt ; \quad 0 \leq y \leq h , \quad x = 0 \qquad (2.16)$$

Equations (2.15) and (2.16) are solved numerically for the crack opening displacements and the dislocation densities. The procedure is discussed in detail in the next section.

3. Numerical Analysis

The procedure for obtaining numerical results for the shear pullout of the rigid insert problem is discussed first. The governing integrodifferential equation, (2.6), and the equation of equilibrium, (2.10), are normalized by introducing the following variable changes:

$$y = \frac{1}{2}\, h(\bar{y} + 1) \;; \quad t = \frac{1}{2}\, h(\bar{t} + 1) \tag{3.1}$$

The function D(t) is non-dimensionalized and given appropriate square root singularities at its ends by making the following substitution:

$$D(t) = \frac{2P}{h}\, \bar{D}(\bar{t})(1 - \bar{t}^2)^{-0.5} \tag{3.2}$$

With these changes, equations (2.6) and (2.10) take on the following forms:

$$\int_{-1}^{1} \frac{\bar{D}(\bar{t})(1-\bar{t}^2)^{-0.5}}{\bar{t} - \bar{y}} dt + \int_{-1}^{1} \bar{D}(\bar{t})(1-\bar{t}^2)^{-0.5} \quad \bar{K}(\bar{y},\bar{t}) d\bar{t}$$

$$= \frac{2\pi(\kappa+1)\mu}{\kappa k_s h} \frac{\partial}{\partial \bar{y}} [\bar{D}(\bar{y})(1-\bar{y}^2)^{-0.5}] \;; \quad x = 0, \quad -1 \le \bar{y},\ \bar{t} \le 1 \;; \tag{3.3}$$

$$\int_{-1}^{1} \bar{D}(\bar{t})(1-\bar{t}^2)^{-0.5}\, d\bar{t} = 1 \;; \quad x = 0, \quad -1 \le \bar{t} \le 1 \tag{3.4}$$

The function $\bar{K}(\bar{y},\bar{t})$ is as given next:

$$\bar{K}(\bar{y},\bar{t}) = \frac{1}{2\kappa} [- \frac{(\kappa-1)^2}{\bar{y}+\bar{t}+2} + \frac{2[2(\bar{t}+1)-\kappa(\bar{y}+\bar{t}+2)]}{(\bar{y}+\bar{t}+2)^2} - \frac{8(\bar{y}+1)(\bar{t}+1)}{(\bar{y}+\bar{t}+2)^3}] \tag{3.5}$$

The spring constant k_s is estimated from the mechanical properties of adhesive

materials representative of the ones used in industry [3]. A simple dimensional analysis carried out on eqn (2.1) shows that the appropriate units for the equivalent spring constant are [force/(length)^3]. If G is the shear modulus of the adhesive and t is its average thickness when applied to such materials as aluminum or titanium alloys, then k_s is given by:

$$k_s = \frac{G}{t} \tag{3.6}$$

Numerical results were obtained for several values of k_s. The range of values considered was based on two adhesives which are used in industry. Their properties will be discussed in the next section.

The kernel of the right-hand side of eqn (3.3) has a Cauchy-type singularity. The numerical method introduced by Gerasoulis and Srivastav [4], [5] is used here to reduce the right-hand side of (3.3) to a system of linear algebraic equations. The method consists of replacing the integral equation by integral relations at a set of points. Piecewise linear functions are then used to approximate the integrand at a finite set of (collocation) points. The values of the unknown function at those points are then obtained via closed form integration.

Equation (3.3) is thus reduced to a system of linear algebraic equations which may be written in matrix form as follows:

$$\frac{1}{c_1} [A] \{\bar{D}(\bar{t})\} = - \{\frac{\partial}{\partial \bar{y}} [\bar{D}(\bar{y})(1-\bar{y}^2)^{-0.5}]\} \tag{3.7}$$

Here, the symbol [ ] denotes a two-dimensional matrix, while { } denotes a column matrix. The integration points $\bar{t}_k$, k=1, 2, ..., 2N+1, are chosen to be equally spaced in the interval $-1 \leq \bar{t}_k \leq 1$, and the collocation points $\bar{y}_j$ are

chosen in the same interval such that $\bar{t}_j \leq \bar{y}_j \leq \bar{t}_{j+1}$, $j=1, 2, \ldots, 2N$. The matrix A contains the coefficients of the unknowns $\bar{D}(\bar{t}_k)$ and they are as given in [5]. The constant c_1 is given by

$$c_1 = \frac{2\pi(\kappa+1)\mu}{\kappa k_s h} \tag{3.8}$$

The solution is obtained using an iterative method. As a first approximation, $\bar{D}(\bar{t}_k)$ are set equal to the results obtained from the solution of the problem which assumes that the insert is <u>perfectly</u> bonded to the half plane, i.e., the case where the spring stiffness k_s tends to infinity. Simple matrix multiplication leads to numerical values for the slopes of the normalized stress discontinuities at the collocation points $\bar{y}_j$. These results are fitted using cubic splines, and then numerically integrated using Gauss' formula (see, e.g., [10], [11]) to obtain values for $\bar{D}$ at $\bar{t}_k$. These values are normalized so that the equilibrium equation (3.4) is satisfied, and the results are substituted back into eqn (3.7) for the next iteration. This process is repeated until a convergence criterion is satisfied. Upon convergence, the results are used to compute the stresses generated in the contact region. The shear stresses are obtained from eqn (3.2). To compute the normal stresses, equation (2.11) is first normalized using eqns (3.1) and (3.2); this yields the following expression:

$$\tau_{xx}(\bar{y}) = \frac{P}{h}\frac{(\kappa-1)}{\pi(\kappa+1)}\left\{\int_{-1}^{1}\frac{\bar{D}(\bar{t})(1-\bar{t}^2)^{-0.5}d\bar{t}}{\bar{t}-\bar{y}}\right.$$

$$\left.+\int_{-1}^{1}\bar{D}(\bar{t})(1-\bar{t}^2)^{-0.5}L(\bar{y},\bar{t})d\bar{t}\right\}\ ; \quad x = 0, \ -1 \leq \bar{y} \leq 1 \tag{3.9}$$

The function $L(\bar{y},\bar{t})$ is given by

$$C(\bar{y},\bar{t}) = \frac{1}{\kappa-1}\left[\frac{3\kappa-1}{\bar{y}+\bar{t}+2} + \frac{2[3(\bar{t}+1)-\kappa(\bar{y}+1)]}{(\bar{y}+\bar{t}+2)^2} - \frac{8(\bar{y}+1)(\bar{t}+1)}{(\bar{y}+\bar{t}+2)^3}\right] \tag{3.10}$$

Equation (3.9) may now be written as a system of linear algebraic equations exactly as it was done with the left hand side of eqn (3.3). Numerical values for the normal stresses at collocation points are obtained by multiplying the matrix of the coefficients of this system of equations by the solution vector $\{\bar{D}(\bar{t})\}$.

The Gerasoulis-Srivastav technique [4] is also used to obtain numerical results for the opening case. First, equation (2.15) is normalized and the dislocation densities are given appropriate singularities at the ends by making the following substitutions:

$$y = \frac{1}{2}h(\bar{y}+1) \;;\quad t = \frac{1}{2}h(\bar{t}+1) \;;\qquad \text{(restated)} \tag{3.1}$$

$$B(t) = \frac{p}{\mu h}\bar{B}(\bar{t})(1-\bar{t}^2)^{-0.5} \tag{3.11}$$

With these substitutions, equation (2.15) becomes:

$$\int_{-1}^{1}\frac{\bar{B}(\bar{t})(1-\bar{t}^2)^{-0.5}d\bar{t}}{\bar{t}-\bar{y}} + \int_{-1}^{1}\bar{B}(\bar{t})(1-\bar{t}^2)^{-0.5}$$

$$\left[\frac{1}{(\bar{y}+\bar{t}+2)} + \frac{2(\bar{t}+1)(\bar{y}-\bar{t})}{(\bar{y}+\bar{t}+2)^3}\right]d\bar{t} = \frac{\pi(\kappa+1)}{2}\frac{h}{p}\left[-\tau_{xx}(0,\bar{y})\right.$$

$$\left. + k\left(\frac{COD}{2}\right)\right] \;;\quad x = 0,\quad -1 \le \bar{y} \le 1 \tag{3.12}$$

The equivalent spring constant for the adhesive in tension, k, is given by the following relation:

$$k = \frac{E}{t} \tag{3.13}$$

Numerical results were obtained for values of E corresponding to the range of G values used in the shear case. A detailed discussion of this is presented in the results and discussion section.

Equation (3.12) is reduced to a system of linear algebraic equations [4], and then placed in matrix form as follows:

$$[M]\ \{\bar{B}(\bar{t})\} = c_2\{-\tau_{xx}(0,\bar{y}) + k(\frac{COD}{2})\} \tag{3.14}$$

The matrix [M] contains the coefficients of the unknown normalized dislocation densities, and c_2 is given as

$$c_2 = \frac{\pi(\kappa+1)}{2}\frac{h}{P} \tag{3.15}$$

Premultiplication of both sides of eqn (3.14) by the inverse of [M] leads to the following relation:

$$\{\bar{B}(\bar{t})\} = c_2[M]^{-1}\ \{-\tau_{xx}(0,\bar{y}) + k(\frac{COD}{2})\} \tag{3.16}$$

The solution for this equation is also obtained via an iterative method. A first estimate of the values in the column matrix $\{-\tau_{xx}(0,\bar{y}) + k(\frac{COD}{2})\}$ is made by setting them equal to some percentage of the opening pressures $\tau_{xx}(0,\bar{y})$. The matrix multiplication indicated at the right-hand side of eqn (3.16) leads to the initial estimate for the dislocation densities $\bar{B}(\bar{t}_k)$. These values are next used to compute the corresponding crack opening displacements from eqn (2.16). First, equation (2.16) is normalized by making the substitutions

given in (3.1) and (3.11). The resulting expression may be written in the following form:

$$\frac{1}{2}\,[\mathrm{COD}]_\alpha = \frac{1}{2}\,[u_x^{(2)} - u_x^{(1)}]_\alpha = -\frac{p}{4\mu}\int_\alpha^1 \bar{B}(\bar{t})(1-\bar{t}^2)^{-0.5}d\bar{t} \; ; \; -1 \leq \alpha \leq 1 \tag{3.17}$$

The values of $\frac{1}{2}$(COD) are needed at the collocation points $\bar{y}_J$. Values of $\bar{B}(\bar{t})$ have been calculated at the integration points $\bar{t}_K$; these values are numerically interpolated using cubic splines. Then, by setting $\alpha = \bar{y}_J$, Gaussian integration leads to the desired values of $\frac{1}{2}$(COD) at $\bar{y}_J$. These results are then substituted into the right-hand side of (3.16) for the next iteration. This procedure is repeated until a convergence criterion is satisfied.

4. Results and Discussion

The numerical analysis was carried out for N = 9 and N = 17, corresponding to 19 and 35 integration points, respectively. There was no significant difference between the two sets of results. The applied load P and the depth h were set equal to 1 for all cases. Results were obtained for a range of tensile and shear elastic moduli E and G. The values considered were set according to the properties of two commercially available adhesives. The first is a relatively rigid one, known as FM-73, manufactured by American Cyanimid, Bloomingdale Division. It is an elastomer modified epoxy material. Its properties were experimentally determined by the Kearfott Division of Singer [12]. The second adhesive material is of relatively low rigidity; it is an experimental one component urethane adhesive produced by Goodyear coded AX37J922 [13]. The average value of G for FM 73 is given in [12] as 84,000 psi. The corresponding value for the Goodyear urethane system is 15,000 psi [13]. Average values for the installed adhesive thickness, t, are given as 0.0047 inches (FM 73) and 0.005 inches (AX37J922). Thus, following eqn (3.6) the corresponding k_s values are 1.789×10^7 lbs/in^3 and 0.3×10^7 lbs/in^3, respectively.

The value of E for the AX37J922 adhesive is given as 43,600 psi [13]. This makes the ratio E/G equal to 2.907. Poisson's ratio for this material is approximately equal to 0.45. These values are in good agreement with the theoretical relation between E, G, and ν:

$$E = 2(1+\nu)G \qquad (4.1)$$

However, the experimentally computed value of E for FM 73 [12], does not

correspond to the value given for G; the average values reported are E = 360,000 psi, G = 84,000 psi. When these values are substituted in eqn (4.1), the resulting value for ν is 1.14. Since ν cannot be greater than 0.5, the value used for E in this case was adjusted to be consistent with the one for the shear modulus. Taking ν = 0.35 and G = 84,000 psi, equation (3.14) gives E = 226,000 psi. The average adhesive thickness t is given as 0.0045 inches for FM 73, and as 0.005 inches for AX37J922. Thus, the corresponding k values are 5.022×10^7 lbs/in^3 and 0.872×10^7 lbs/in^3, respectively. Numerical results were obtained for four intermediate sets of k_s, k values equally spaced between the ones already given, as well as for two sets of k_s, k values one lower than the AX37J922 ones, and the other higher than the FM 73 ones. The values used are given in Table 1.

Table 1. Shear and Tensile Spring Constants

Code	k_s (lbs/in^3)	k (lbs/in^3)
A	0.0022×10^7	0.042×10^7
B	0.3000×10^7	0.872×10^7
C	0.5878×10^7	1.702×10^7
D	0.8956×10^7	2.532×10^7
E	1.1934×10^7	3.362×10^7
F	1.4912×10^7	4.192×10^7
G	1.7890×10^7	5.022×10^7
H	2.0868×10^7	5.852×10^7

Two adherend materials were considered: The 7075-T6 aluminum alloy and the Ti-6Al-4V titanium alloy. Both of these materials find widespread application in aircraft structures. Material constants for the aluminum alloy are taken as E = 10.4×10^6 psi, μ = 3.75×10^6 psi, and ν =0.33; the ones for the titanium are E = 16×10^6 psi, = 6.4×10^6 psi, and ν = 0.34. All results

plotted here are the ones obtained for the plane strain case with N = 17, and with Ti-6Al-4V being the adherend material.

The normalized shear stress distribution generated during the shear pull-out of the insert is plotted in Figure 2 for all k_s values considered, as a function of the (non-dimensionalized) distance from the free surface. As given in Table 1, the curve identified by A corresponds to the case where the adhesive has the least rigid shear spring constant $k_s = 2.2 \times 10^4$ lbs/in^3. At the other extreme, curve H gives the shear stress distribution for the case where the most rigid adhesive is used. This figure shows that the shear stresses attain their maximum values near the tip of the insert, and that they are smallest near the free surface of the half plane. In the lower limiting case, A, the variation is not detectable and the stresses are constant along the insert. The difference between the shear stresses near the tip and those near the free surface is most pronounced for the case involving the most rigid adhesive. As the rigidity of the adhesive increases these results converge to the ones obtained for the "perfectly bonded" case [6]. It is also interesting to note that the curves seem to "pivot" about a point near which the value of y is approximately 65% of h. This behavior of the shear stresses is predicted by a simple 1-D model analysis.*

These results show that the adhesive will tend to fail (yield) near its tip first. This will result in a redistribution of the stresses along the bond line. This type of non-linear behavior will be investigated in future work.

The non-dimensionalized normal stress distribution is shown in Figure 3 as a function of the normalized distance from the free surface. For clarity,

*This 1-D model comparison was pointed out by Professor P.J. Torvik, Air Force Institute of Technology.

only the two extreme cases are plotted. These figures show that the maximum normal stresses occur near the free surface, and they tend to zero as y approaches h. It is also observed that these stresses vary significantly with k_s only at their extreme values near $y = 0$. There, the stress increases with increasing k_s. Away from $y = 0$, the normal stress distributions seem to be independent of the rigidity of the adhesive.

These results are significant, especially when viewed in light of the shear stress results (Figure 2). When the adhesive fails in shear, initially near the tip, residual compressive stresses, such as those encountered in fiber reinforced composite materials [1], [14], would tend to keep the debonded surfaces in contact, thus inducing friction forces in the failed region. This in turn would tend to counter shear propagation of the crack at the fiber-matrix interface. Since the normal stresses in this region are negligible, the residual stresses would dominate and the crack surfaces would remain in contact. However, as the adhesive's damaged zone increases in length, thus moving away from the tip, the normal stresses increase, and at some distance from the tip they will balance the residual compressive stresses, thus eliminating friction. Beyond that point, the growth of the damaged zone may accelerate under the combined action of the shear stresses and of the opening pressure, until complete debonding is reached. This suggested failure process seems to be in very good agreement with the experimental results obtained by Atkinson, et al. [15] for the axisymmetric case.

The results obtained from the solution of the problem involving the edge crack subjected to opening pressure are plotted in Figure 4. The crack opening displacements are symmetric about the $x = 0$ axis (see Fig 1). The curves shown represent the opening at either side of the insert as a function of (normalized) distance from the free surface. Thus, these are the displace-

ments which are multiplied by the tension spring constant, k, to obtain the resistance to opening due to the adhesive.

These results show that the opening displacements increase with decreasing adhesive stiffness, k. This is what one would expect, considering the opening pressure, τ_{xx}, does not vary substantially for different adhesive materials (k_s), as shown in Figure 3, while the resistance to opening, k(COD/2), increases considerably with increasing k. Thus the magnitude of the right-hand side of eqn (2.15) is very sensitive to the magnitude of k. This is shown in Figure 5, where the "net" opening pressure, $-[-\tau_{xx} + k(\frac{COD}{2})]$, is plotted for all cases as a function of distance from the free surface. This figure shows good agreement between the applied "net" opening pressures (increasing with decreasing k) and the crack opening displacements shown in Figure 4.

It should also be noted that the crack opening displacements near the tip ($y = h$) are between one and two orders of magnitude smaller than the ones near the surface ($y = 0$). This behavior is consistent with the variation in the net opening stresses plotted in Figure 5. Thus, the crack is essentially closed over a portion of its length near the tip of the insert, and the length of the closed segment increases with k. It should be emphasized here that this analysis does not account for any residual compressive stresses that may be introduced during the manufacturing processes. The presence of any such stresses would clearly tend to increase the length over which the crack is closed.

Acknowledgements

The authors are grateful for support from the Frank J. Seiler Research Laboratory (U.S. Air Force). Portions of this investigation were completed while G.K. Haritos was at the Department of Engineering Mechanics, U.S. Air Force Academy. The authors are grateful to Mr. H.S. Schwartz of the Air Force Wright Aeronautical Laboratories for providing them with data for adhesive materials. L.M. Keer is grateful for partial support from the National Science Foundation, Grant No. MEA 8117106.

LIST OF SYMBOLS

A, B, C, D, E, F, G, H	Adhesive Materials Designations
A	Coefficient Matrix
B(y)	Dislocation Densities
c_1, c_2	Constants
COD	Crack Opening Displacements
D(y)	Stress Discontinuities
E	Young's Modulus
G	Shear Modulus of Adhesive Materials
h	Embedded Length of Insert
k	Equivalent Adhesive Spring Constant (Tension)
k_s	Equivalent Adhesive Spring Constant (Shear)
K(y,t); L(y,t)	Integrand Functions
M	Coefficient Matrix
N	Half the Number of Collocation Points
P	Applied Load
t	Adhesive Thickness
u_o	Rigid Insert Displacement
u_x, u_y	Half Space Displacements
x, y	Coordinates
κ	Half Space Material Constant
μ	Half Space Shear Modulus
ν	Poisson Ratio
τ_{xx}, τ_{xy}	Normal and Shear Stresses
τ_{xx}^{c}	Crack Opening Pressure

References

Code

[1] Brussat, T.R. and Westmann, R.A., Interfacial Slip Around Rigid Fiber Inclusions, J. Composite Materials, Vol 8, 364, 1974.

[2] Chamis, C.C., Mechanics of Load Transfer at the Interface, in Composite Materials (Broutman, L.J., and Krock, R.H., editors), Vol 6, Academic Press, NY 1974.

[3] Potter, D.L., Primary Adhesively Bonded Structure Technology (PABST), AFWAL-TR-80-3112, November 1980.

[4] Gerasoulis, A. and Srivastav, R.P., A Method for the Numerical Solution of Singular Integral Equations with a Principal Value Integral, Int. J. Engng. Sci., Vol 19, 1293, 1981.

[5] Gerasoulis, A., The Use of Piecewise Quadratic Polynomials for the Solution of Singular Integral Equations of Cauchy Type, Computers and Mathematics with Applications, 8(1), 15, 1982.

[6] Haritos, G.K. and Keer, L.M., Stress Analysis for an Elastic Half Space Containing an Embedded Rigid Block, Int. J. Solids Structures, Vol 16, 19, 1980.

[7] Keer, L.M. and Chantaramungkorn, K., An Elastic Half Plane Weakened by a Rectangular Trench, J. Appl. Mech., Vol 42, 683, 1975.

[8] Sneddon, I.N., The Use of Integral Transforms, McGraw-Hill, NY, 1972.

[9] Erdelyi, A., (ed), Tables of Integral Transforms, Vol I, McGraw-Hill, NY, 1954.

[10] Stroud, A.H. and Secrest, D., Gaussian Quadrature Formulas, Prentice-Hall, Englewood Cliffs, NJ, 1966.

[11] Abramowitz, A. and Stegun, I.A., Handbook of Mathematical Functions, Dover, NY, 1965.

[12] Hughes, E.J. and Rutherford, J.L., Selection of Adhesives for Fuselage Bonding, Final Report No. KD-75-37, 1975, The Singer Company, Kearfott Division.

[13] Goodyear Chemicals Advance Tech Data, August 1979, Goodyear Rubber and Tire Company, Akron, Ohio.

[14] Broutman, L.J., Mechanical Requirements of the Fiber-Matrix Interface, J. Adhesion, Vol 2, 147, 1970.

[15] Atkinson, C., Avila, J., Betz, E. and Smelser, R.E., The Rod Pull Out Problem, Theory and Experiment, J. Mech. Phys. Solids, Vol 30, 97, 1982.

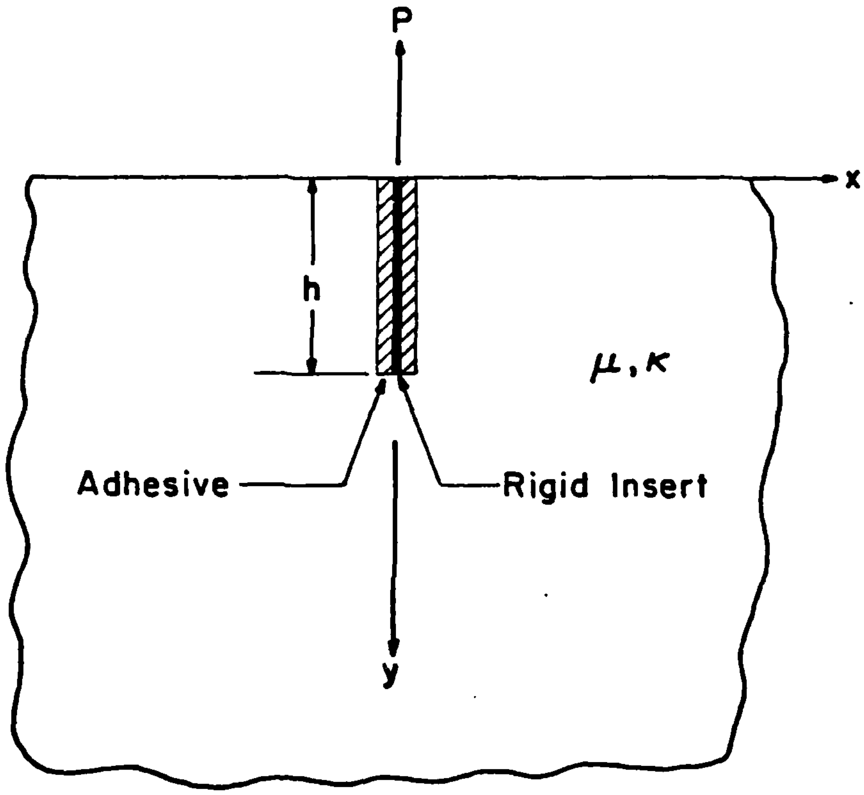

Fig. 1 Geometry and coordinate system for a partially embedded finite rigid insert undergoing shear displacement.

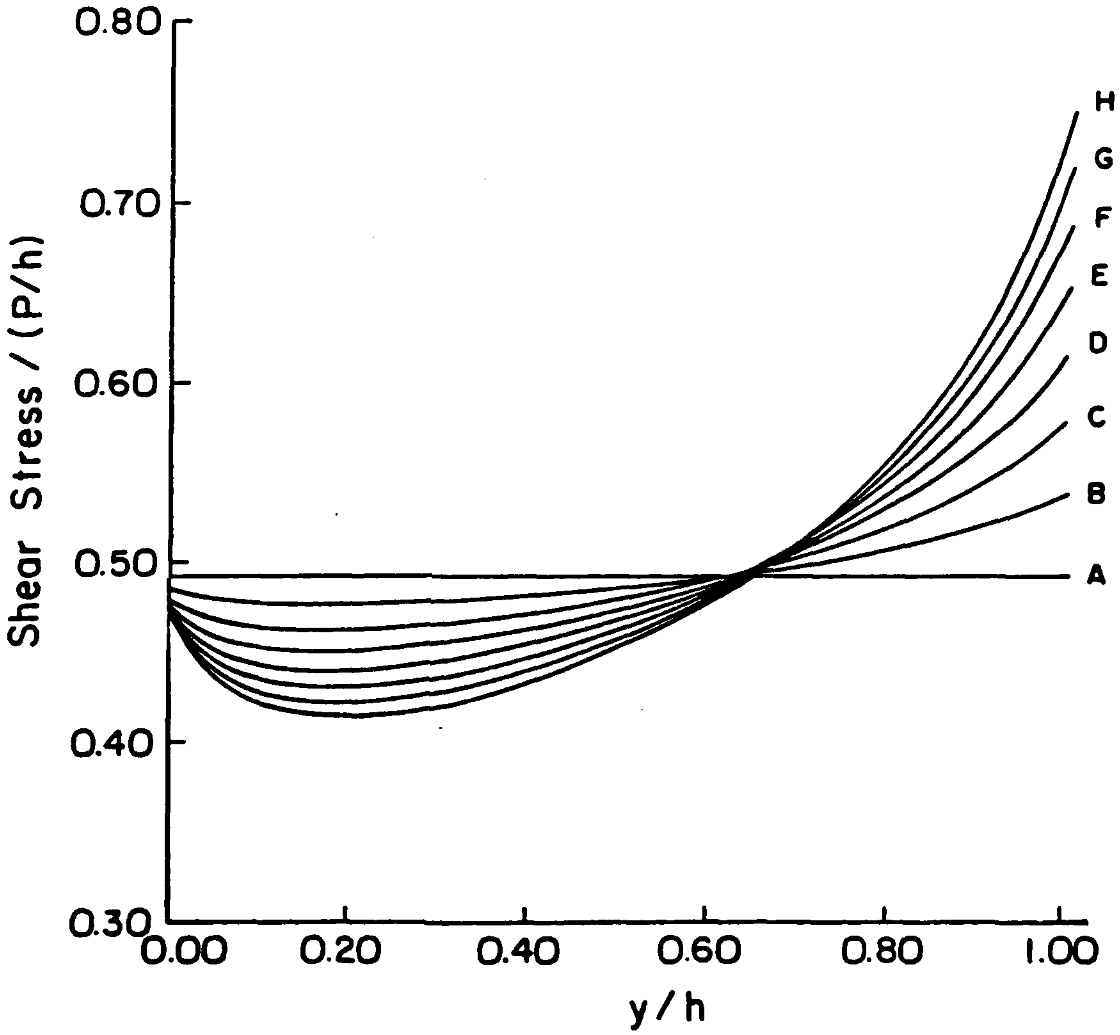

Fig. 2 Shear Stress Distribution at x=0 for the shear pullout problem.

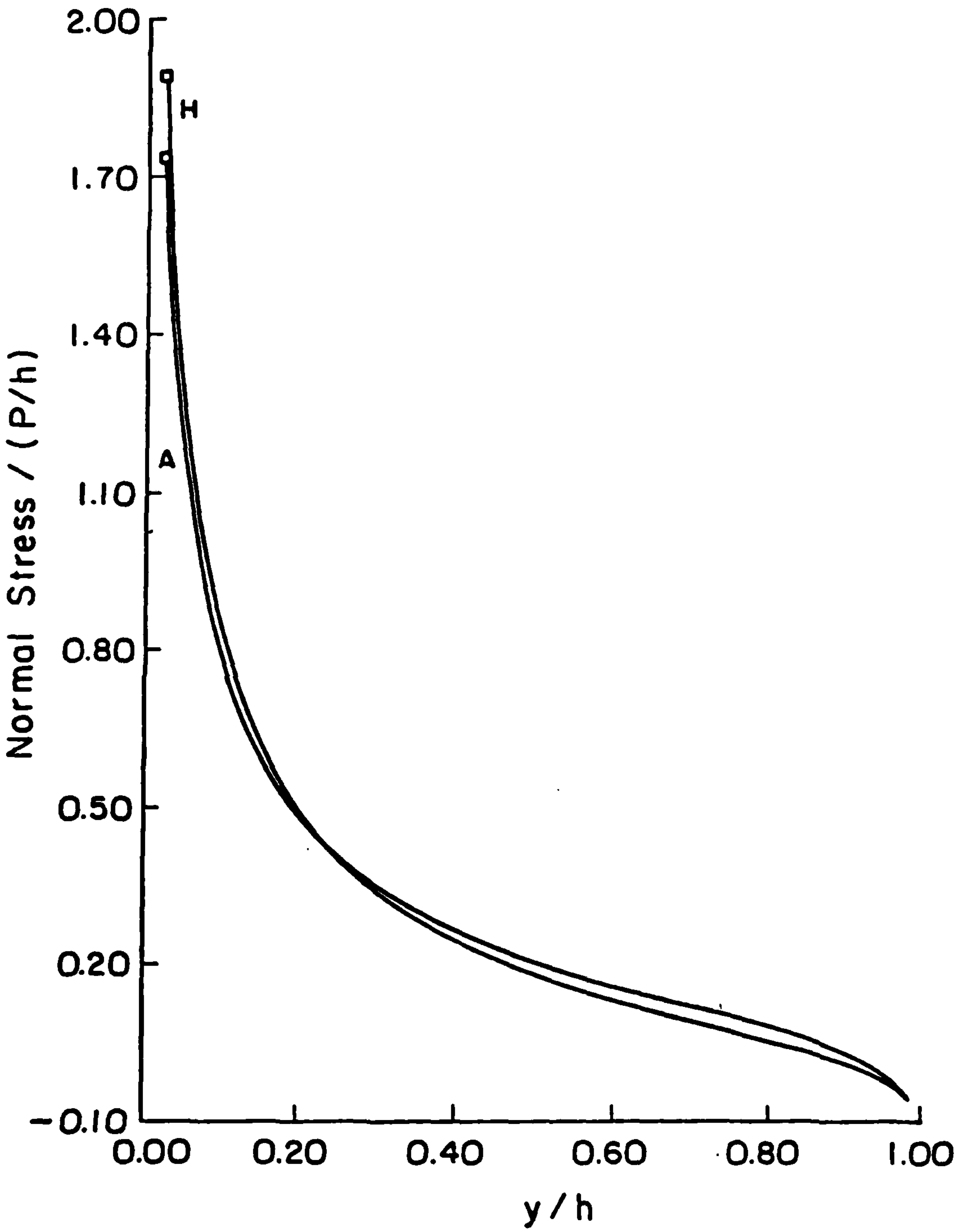

Fig. 3 Normal Stress Distribution at x=0 for the shear pullout problem (maximum and minimum k_s only).

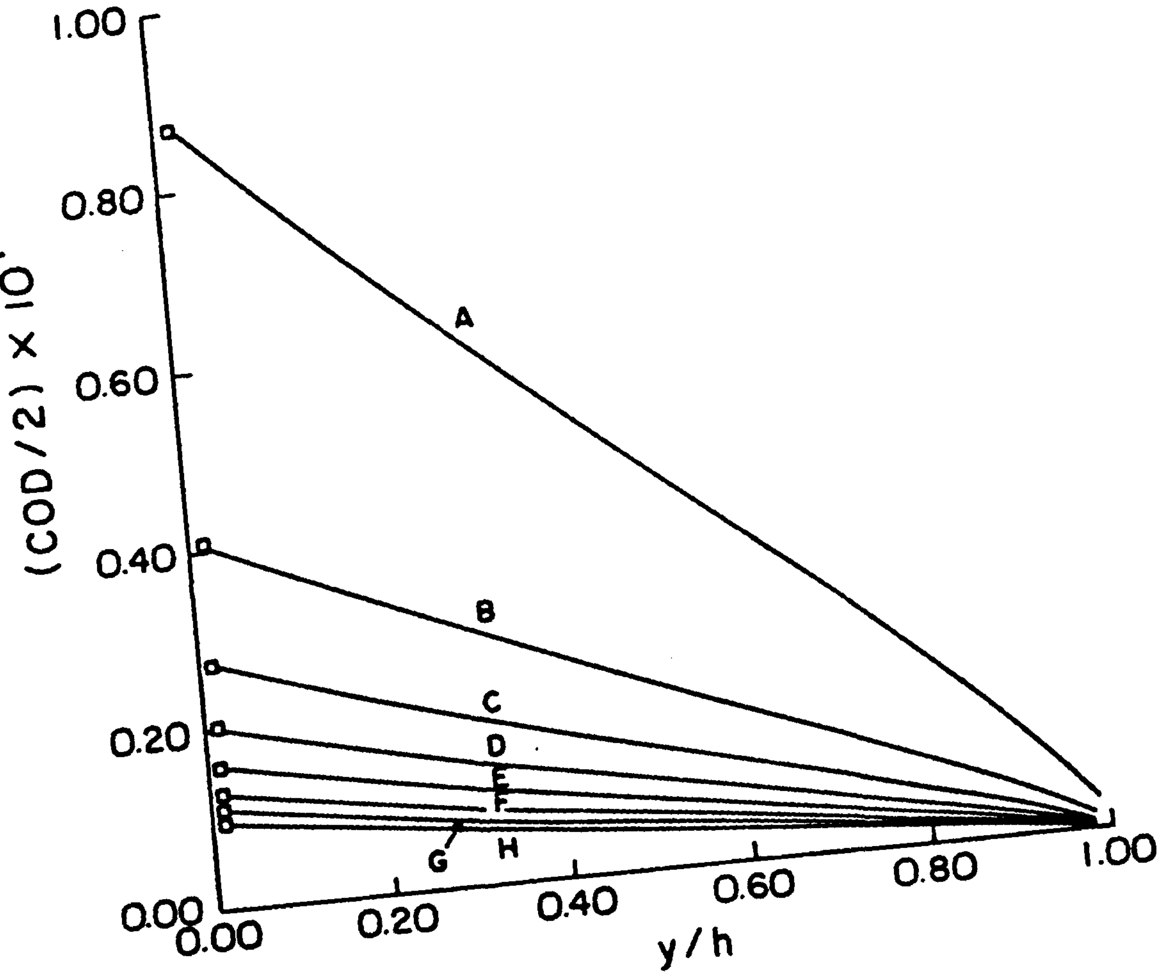

Fig. 4 Crack Opening Displacements at x=0 for the opening problem.

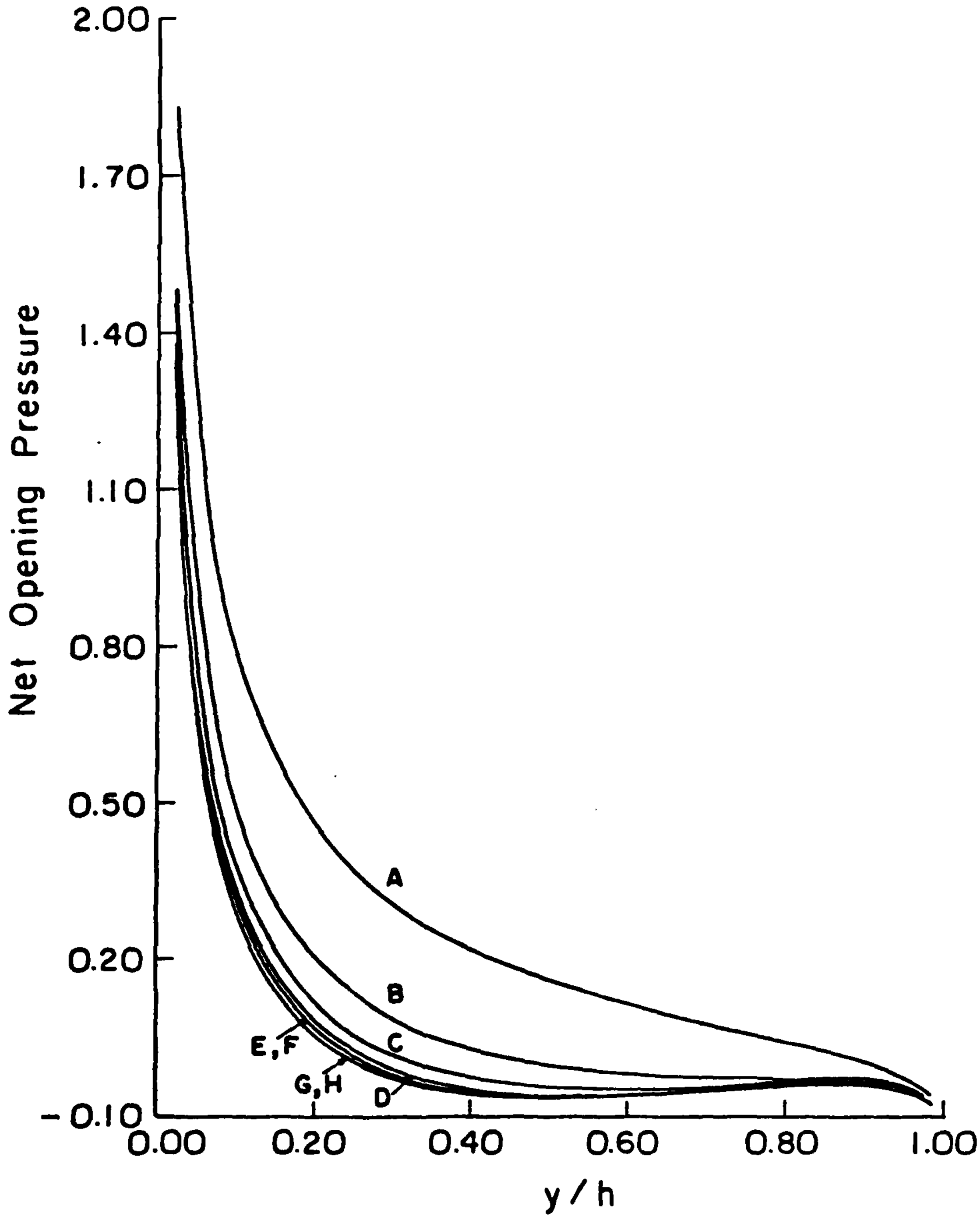

Fig. 5 Net Opening Pressure [τ_{xx} - k .($\frac{COD}{2}$)] at x=0 for the opening problem.

FILM

3-8